Editor's Choice

Atomic force microscopy study of hexagonal boron nitride film growth on 6H-SiC (0001)

Wei Chen[1], **Kian Ping Loh**[*, 1], **Ming Lin**[1], **Rong Liu**[2], and **Andrew T. S. Wee**[2]

[1] Department of Chemistry, National University of Singapore, 3 Science Drive 3, Singapore 117543
[2] Department of Physics, National University of Singapore, 2 Science Drive 3, Singapore 117542

The growth of hexagonal Boron Nitride films (*h*-BN) on 6H-SiC (0001) using plasma-excited borazine has been studied. On 6H-SiC (0001), the growth of pin-hole free, compact *h*-BN film is difficult due to poor wetting properties between *h*-BN and 6H-SiC. The strained BN layer releases its elastic energy by a morphological instability at the interface. This strain relief mechanism gives rise to a buckling of the film into longitudinal islands and round trenches between 500–700 °C. At 300 and 900 °C however, the strained islands can attain their minimum-energy size to form homogeneously-sized spherical islands with diameter of ~500 nm. Compositional analysis of the BN films grown at 900 °C using XPS shows that these are actually BC_xN film with $x \sim 0.15$, whereas the films grown at 300 °C have less carbon incorporation but higher O content.

1 Introduction

Beside its high-temperature stability, chemical inertness and hardness, boron nitride (BN) also exhibits potential applications [1–4] as UV-detectors, cold cathode materials, and gate-insulators for metal–insulator-semiconductor field-effect-transistors (MISFETs). There have been numerous attempts to use borazine as a single-precursor for the growth of boron nitride thin films. The initial stages of borazine adsorption on metal surfaces such as Ni(100) [5–8] and Rh(111) [9] have been investigated recently. It is found that defect-free h-BN monolayer grows on Ni(100) because of good lattice-matching, and the phonon dispersion of the monolayer BN film had been recorded [5–8]. On the other hand, highly regular BN nanomeshes are formed on Rh(111) due to the intrinsic stress caused by the 6.7% lattice mismatch between Rh(111) and h-BN [9]. This BN nanomesh can be used as a template for the mono-dispersion of metallic nanoparticles, or in the corner-site directed growth of fullerenes. In this work, we address the growth of hexagonal BN films on another hexagonal substrate, 6H-SiC (0001). The incommensurate lattice unit cell coupled with the chemical non-reactivity of BN and SiC would suggest that the nucleation and growth of high quality film may be difficult; nevertheless this provides an opportunity to study the nucleation kinetics of BN on an inert substrate. The dielectric properties of BN depend on its composition and crystallinity. Crystalline BN films for example have a higher relative dielectric constant ($\varepsilon_{BN} = 7.1\ \varepsilon_0$) compared to SiO_2 ($\varepsilon_{SiO_2} = 3.9\ \varepsilon_0$). One possible application is the fabrication of BN films on 6H-SiC substrates as gate insulators in SiC-based MISFET devices. On the other hand, amorphous BC_xN films was found to be a low dielectric constant material with $k = 2.4$, and is useful as intermetallic dielectrics.

[*] Corresponding author: e-mail: chmlohkp@nus.edu.sg, Phone: +65 6874 4402, Fax: +65 6779 1691

The presence of carbon in 6H-SiC may influence the composition of the films at the interface. Motivated thus, we performed atomic force microscopy (AFM) and secondary ion mass spectrometry (SIMS) studies of *h*-BN film growth on 6H-SiC.

2   Experiment

The growth of BN thin films on 6H-SiC(0001) was carried out in an Astex plasma enhanced chemical vapor deposition (PECVD) chamber equipped with a 2.45 GHz remote discharged microwave plasma source. Borazine ($B_3N_3H_6$) carried by H_2/N_2 was used as the single-precursor for BN film growth. A n-type 6H-SiC(0001) sample, supplied by CREE Research Inc, was used in our experiment. The BN films were grown at different substrate temperatures whilst keeping the other parameters constant. The flow rates were regulated at 40 sccm of N_2, 20 sccm of H_2 and 5 sccm of borazine. The chamber pressure during the film growth was fixed at 25.0 torr, the plasma power at 400 W, and the growth time at around 10 mins. The surface mophorlogy and roughness for the as-grown BN thin films were characterized by AFM (PSIA Inc, Korea) using non-contact mode and dynamic force mode. X-ray photoelectron spectroscopy (XPS) measurements were taken using an Mg X-ray anode (1253.6 eV) at constant analyzer pass energy of 10 eV. Sputtering of the samples was carried using an Ar^+ ion gun at an energy of 2 keV. All depth profiles of the BN films grown on SiC surface were performed with a Cameca IMS 6f SIMS instrument using an O_2^+ primary beam of 1.3 keV.

3   Results and discussion

Mirror-shine, blue *h*-BN films could be deposited on 6H-SiC following plasma chemical vapor deposition with borazine. The root-mean-square (r.m.s.) roughness of the films synthesized at 300, 450, 600 and 900 °C, as determined by AFM, are 3.8 nm, 21 nm, 71 nm and 2.6 nm, respectively. At substrate temperatures lower than 450 °C, only amorphous BN films with poor adhesion properties were fabricated. In order to investigate the role of substrate temperature in the growth of BN thin films, all parameters except the substrate temperature were kept constant during the growth. We found that at 300 °C and 900 °C, the films synthesized were very smooth and had similar morphologies, but the growth rate of 2.7 Å/s at 300 °C was higher than the rate of 0.8 Å/s at 900 °C. The film thickness was measured using SIMS and stylus profilometer. The lower growth rate at higher temperature can be explained by the shorter residence time of the BN precursor on the surface due to desorption reactions at higher temperatures.

While the rate of film growth is determined by kinetics, the thermal equilibrium structure of the surface layer is determined by thermodynamics. The morphological evolution of the BN film in the temperature window between 400 to 800 °C observed in this work can be attributed to the changes in both the size and shape of the islands following facilitated aggregation of the BN precursors at higher substrate temperature. Figure 1 displays the AFM images of BN thin films grown on SiC substrates at different temperatures from 300 °C to 900 °C, scanned over a range of 40×40 μm^2. The magnified plane view and 3-D view of the spherical-shaped, regular-sized BN islands grown at 300 °C are shown in Fig. 2(a) and (b). The line profile [Fig. 2(c)] shows that BN spherical islands with a diameter of about 500 nm were synthesized. The root-mean-square surface roughness of the film is about 3.8 nm. Aggregation of these BN islands occurred as the deposition temperature was increased to 450 °C. Figure 3 is the magnified AFM image of the longitudinal islands grown at 450 °C, it can be seen that these longitudinal islands consist of smaller spherical BN aggregates of 500 nm diameter.

Increasing the substrate temperature to 600 °C during growth resulted in larger islands which form circular edge boundaries, as shown by the AFM images in Fig. 4(a)–(d). Interestingly, we observed that the circular domains in Fig. 4 was formed by the aggregation of smaller, longitudinal BN islands. These were in turn formed by the aggregation of BN spherical islands which was observed by the growth at 300 °C. It therefore appears that there is a trend in the morphological transformation from primary to tertiary organization starting from the 500 nm BN spherical building blocks. With increasing substrate

4 μm
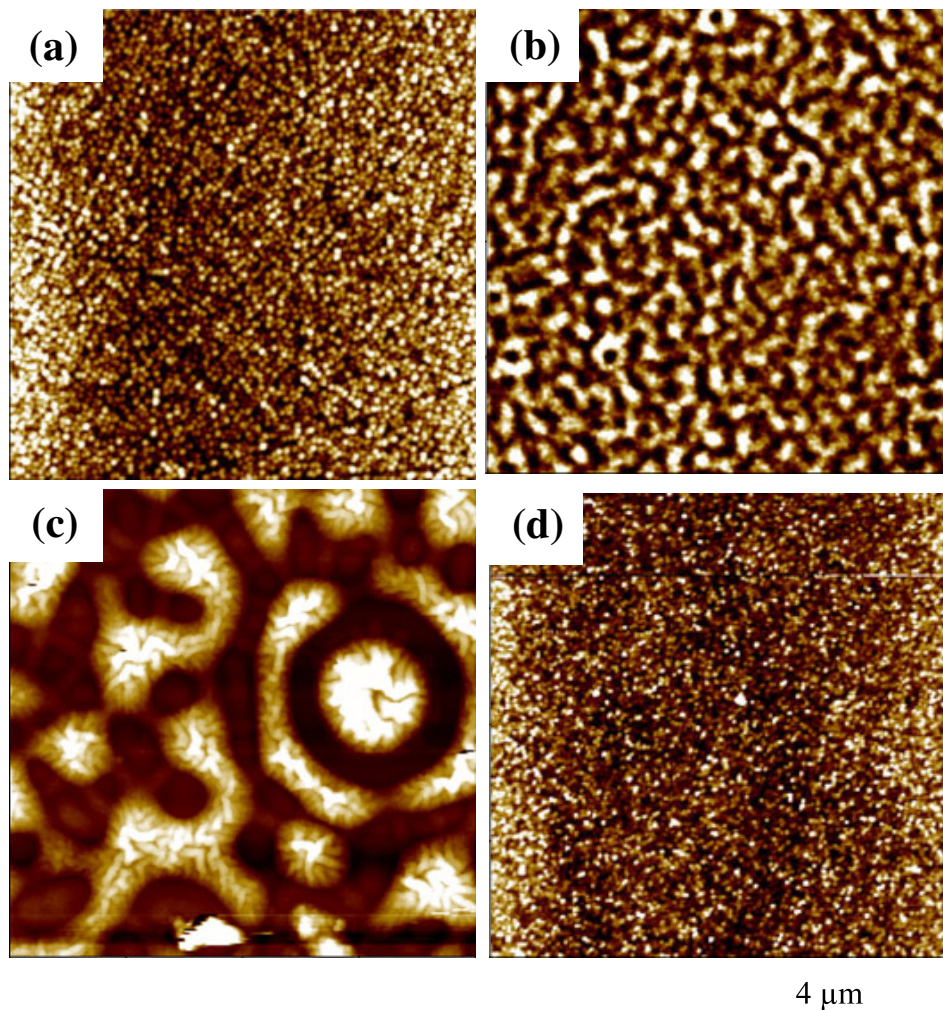
Fig. 1 40×40 μm^2 AFM topographies of the BN film grown on the 6H-SiC substrate by PECVD at temperatures of (a) 300 °C, (b) 450 °C, (c) 600 °C, and (d) 900 °C, respectively.

temperature, the organization is: BN nanoballs → longitudinally-shaped islands consisted of aggregated BN nanoballs → islands with circular boundaries consisted of longitudinal-shaped aggregates. The facilitated diffusion of adatoms at higher temperatures clearly resulted in the growth of islands with larger sizes, however the shape of the islands depends on different stress-relief mechanism. The latter is specific for islands of different sizes due to the need to balance between surface energy, interface energy and energy changes due to elastic relaxation. Interestingly, increasing the growth temperature to 900 °C produced again homogeneously-sized BN nanoballs, as shown in Fig. 5. The diameter of these BN nanoballs was about 300 nm as determined by the line profile measurement in Fig. 5. The RMS roughness of the surface is now only 2.6 nm.

The lattice-mismatch between the 6H-SiC substrate and h-BN film is about 18.86% $\left(f = \dfrac{a(\text{SiC}) - a(h\text{-BN})}{a(\text{SiC})} = \dfrac{3.086 - 2.504}{3.086} = 18.86\% \right)$. Heteroepitaxy produces strained layers due to lattice mismatch between the substrate and the overlayer. In recent years, it has been recognized that strained layers are unstable against shape changes. Shape changes, in addition to dislocation generation, have
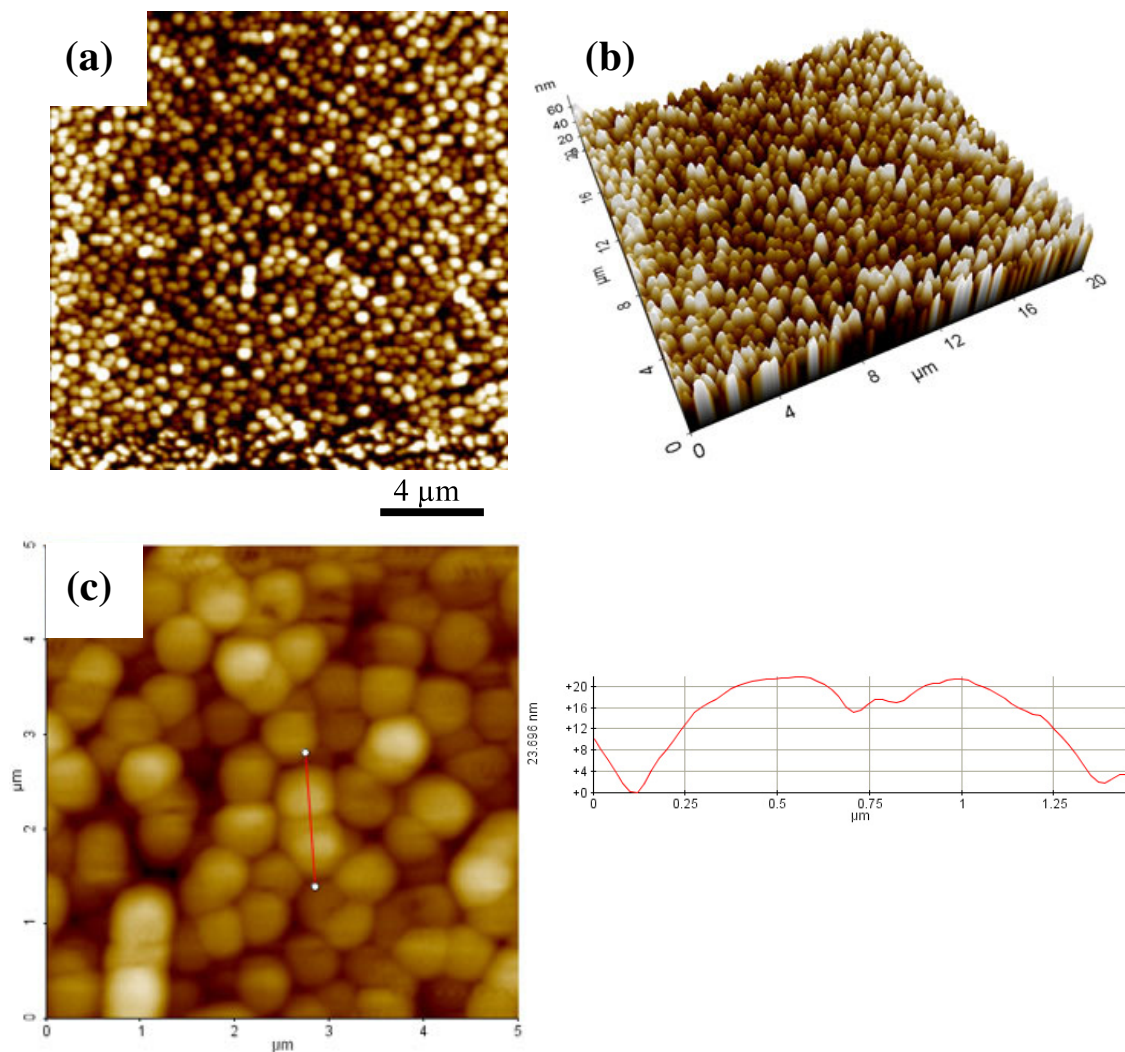
Fig. 2   (a) 20×20 μm^2 AFM image, (b) 3-D AFM image, and (c) the line profile of the BN film grown at 300 °C.

been identified as a major mechanism for strain relief on surfaces that are elastically strained. Tersoff and Tromp [10] showed that strained islands, as they grow in size, may undergo a shape transition from a compact symmetrical shape to elongated shape at larger sizes for better elastic relaxation of island stress. At 300 °C, the homogeneously-sized BN nanoballs as shown in Fig. 2 constitute the thermally equilibrium structure, which is a tradeoff between the surface energy and strain. However as the substrate temperature is increased, the facilitated diffusion of the BN precursor result in aggregation of the BN nanoballs, and these grow beyond its original optimal size. According to Tersoff [10], the trade off between relieving the elastic strain inherent in larger sized islands and the surface energy result in an evolution from spherical islands to elongated islands. The trend we observed in Figs. 3 and 4, where spherical aggregates asssemble to form bigger elongated islands, confirm this. As the islands grow larger, the elongated islands assemble to form domains with circular boundaries. This is the tertiary level of stress relief by surface domain boundaries; the formation of circular boundary is a consequence of minimizing biaxial stress for thicker films. However at even higher temperatures, these big islands are fragmented into smaller BN nanoballs. We believe that above 600 °C, the residence lifetime of the BN precursors on
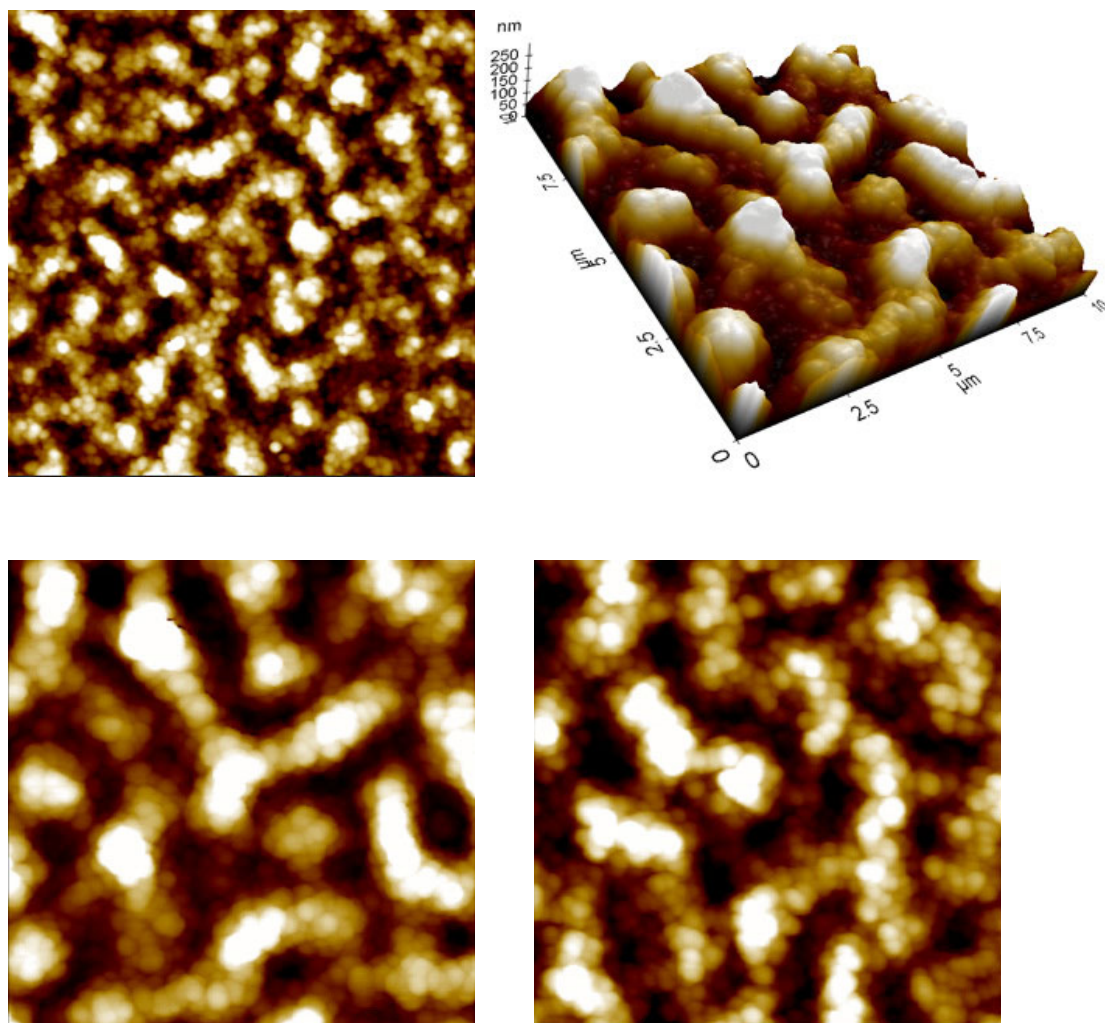
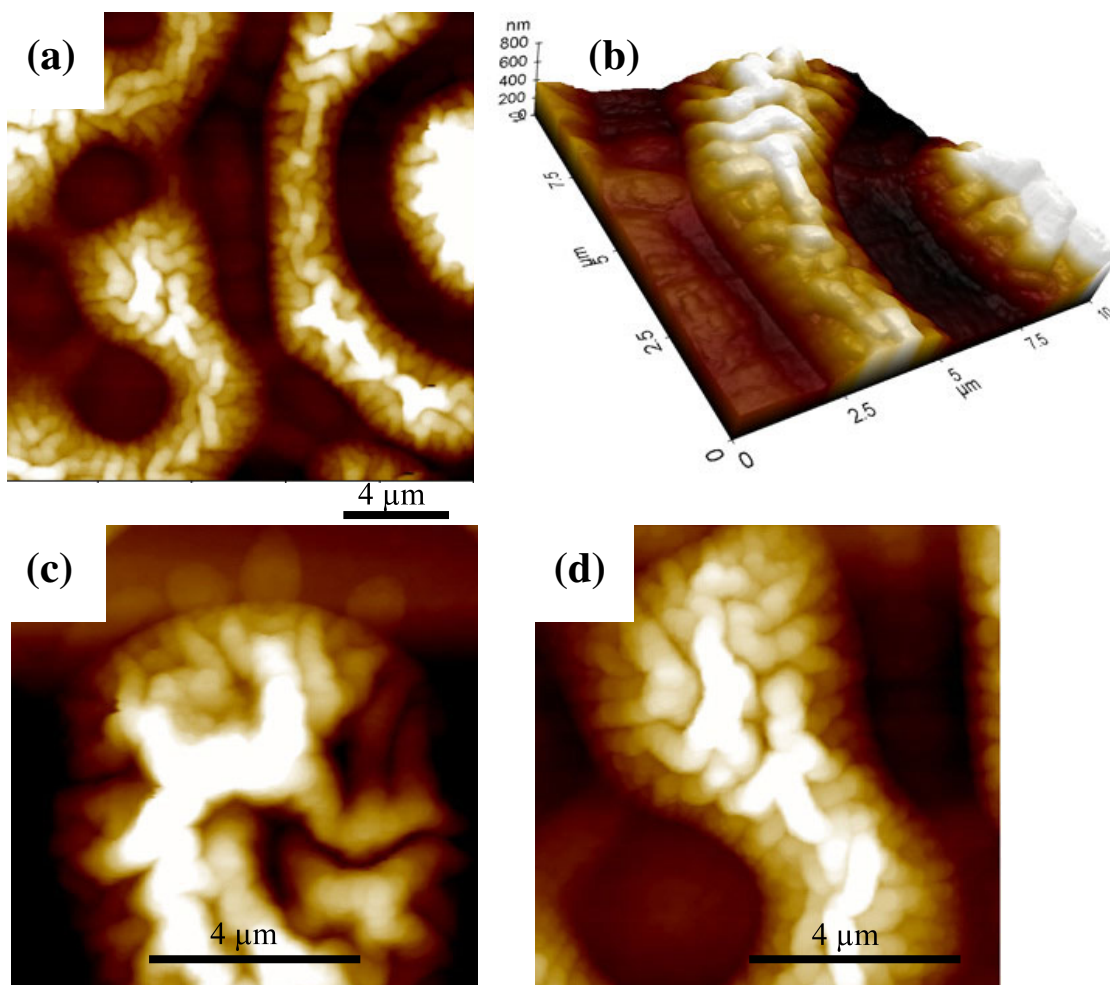**Fig. 3**   (a) $20 \times 20 \ \mu m^2$ AFM image, (b) 3-D AFM image, (c) and (d) magnified $10 \times 10 \ \mu m^2$ AFM images of the BN film grown at 450 °C.

the surface is reduced significantly due to desorption, and coupled with the fragmentation of BN aggregates at this temperature, this will limit the aggregation rate of the spherical islands to form bigger islands. Therefore at high temperature, the strained islands maintained their minimum energy size similar to the islands at 300 °C.

Figure 6 show the SIMS data for the BN thin film grown on SiC surface at 300 °C and 900 °C. We can see the B^+ and N^+ signals extending for about 45 nm to 90 nm before declining at the BN-SiC interface. As shown in Fig. 6(a), significant quantities of oxygen species were trapped at the interface of the BN/SiC for the films grown at 300 °C, this may be due to the presence of residual surface oxide species on SiC. In other words, the growth of the BN film occurred on an oxide-terminated SiC face at lower substrate temperature, this may be responsible for the poor adhesion properties of the BN film on 6H-SiC. Previous experiments on the hydrogen plasma treatment of 6H-SiC shows that despite the fact that there has been no intentional introduction of O into the MWPECVD system, a thin silicon oxide invariably grows on the 6H-SiC surface after H-plasma treatment [11–15] due to the presence of background O in the PECVD chamber (1×10^{-3} torr base pressure). For the BN thin film which was grown on the SiC

Fig. 4 (a) $20 \times 20\ \mu m^2$ AFM image, (b) 3-D AFM image, (c) and (d) magnified $10 \times 10\ \mu m^2$ AFM images of the BN film grown at 600 °C.

surface at 900 °C, the interface shows a significantly smaller quantity (lower by two orders) of oxygen species at the interface, as can be seen in Fig. 6(b). As determined by SIMS, the oxygen content in the as-grown BN thin film at 900 °C was less than 1%. However, another significant difference is the higher degree of carbon incorporation in the BN film grown at 900 °C. Comparing the depth profile of C in Fig 6(a) and (b), the degree of incorporation of C is an order of magnitude higher for films grown at 900 °C.

For all samples grown, the B:N ratio was determined to be 1:1 from XPS and SIMS measurements after taking into account the atomic sensitivity factor (ASF). The B 1s and N 1s XPS peaks in Fig. 7 exhibit a full-width-at-half maximum (FWHM) of 1.35 eV and 1.20 eV respectively. The XPS results for the film grown at 900 °C, however, show that there are about 15% carbon species throughout its depth, such that strictly speaking, the film we synthesized at 900 °C is BC_xN ($x < 1$). At present the origin of this carbon incorporation is not clear. One possibility is the diffusion of carbon from the graphitized SiC surface, since diffusion is enhanced at higher substrate temperature, and the graphitization of SiC surface can proceed at temperatures ≥900 °C. However the relatively constant depth profile of the carbon signals in the BN film rules out diffusion from the bulk since no diffusion gradient of C originating from the interface can be discerned. Other possibilities include the etching of the carbon and silicon species from the SiC surface by the hydrogen plasma since this is used as a carrier gas, the carbon may then be mixed
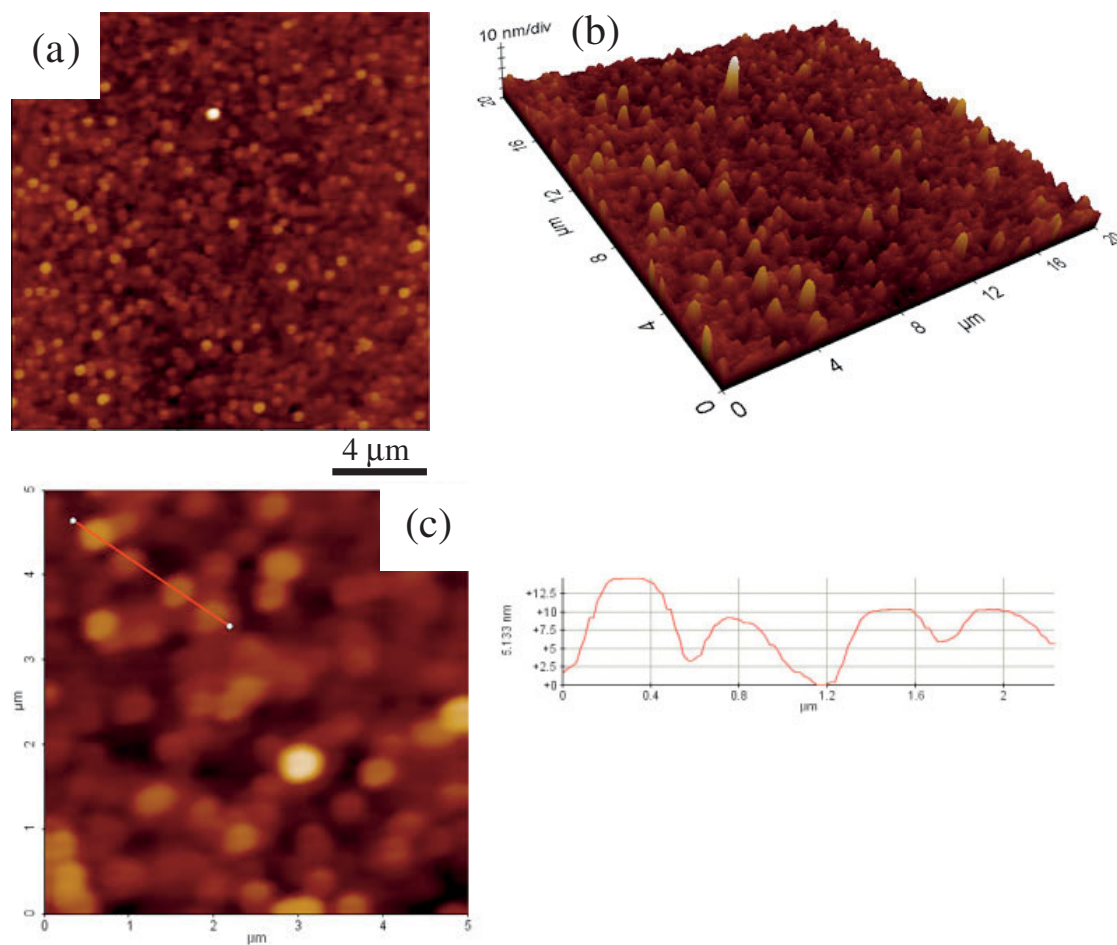
Fig. 5 (a) $20 \times 20 \ \mu m^2$ AFM image, (b) 3-D AFM image, and (c) the line profile of the BN film grown at 900 °C.
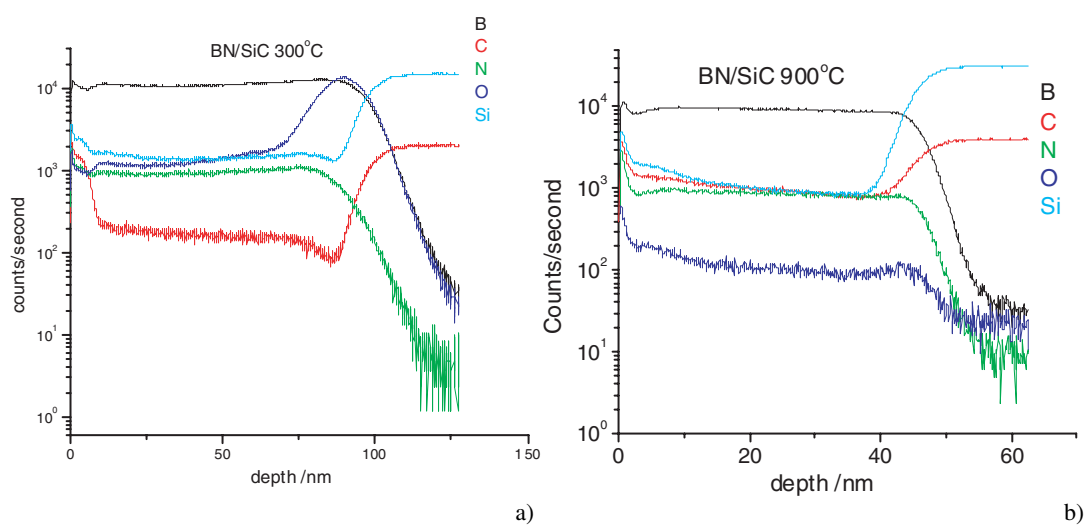
**Fig. 6** SIMS spectra of the BN thin film grown at (a) 300 °C and (b) 900 °C.

© 2005 WILEY-VCH Verlag GmbH & Co. KGaA, Weinheim
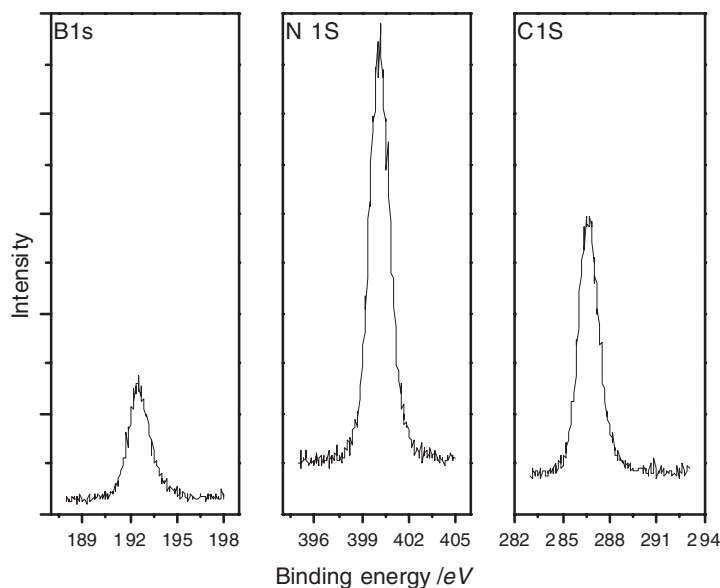
Fig. 7   B 1*s*, N 1*s* and C 1*s* XPS spectra of the BN thin film grown at 900 °C.

with the plasma discharge and incorporated in the growing BN film. If this is the case the carbon concentration should show a decreasing concentration gradient from the interface to the surface since such etching will be blocked after a thicker BN film passivates the surface, but such a concentration gradient is clearly absent in the SIMS spectra. The most likely possibility is due to the graphite heating stage, because at the higher heating temperature of 900 °C, the more efficient plasma etching results in the incorporation of carbon from the graphite stage into the growing BN film, producing a homogeneous BC_xN film. Figure 8 displays the Raman spectra for the as-grown BC_xN thin film at 900 °C. A peak located at 1367 cm^{-1} is attributed to the sp^2-hybridized BN species.

4   Conclusion

Atomic Force Microscopy has been used to study the growth morphologies of BN films on 6H-SiC. The growth at 300 °C proceeded on an oxide-rich interface as revealed by SIMS. At temperature windows between 400–700 °C, the BN film exhibits morphological instability and micron-sized stress-relief fea-
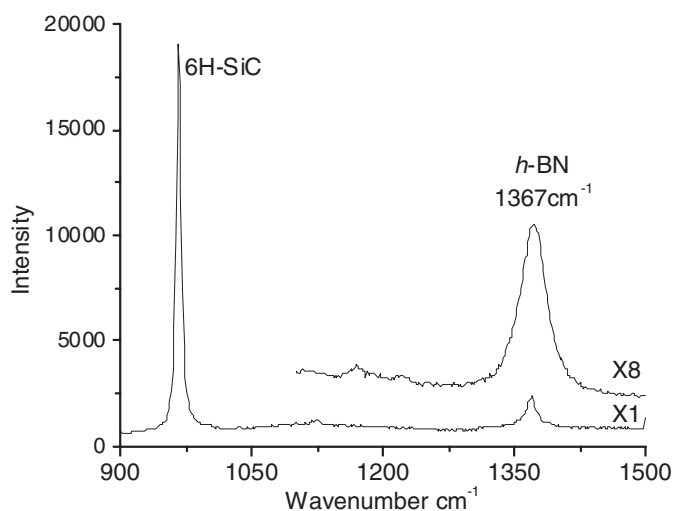
Fig. 8   Raman spectrum of the BN thin film grown at 900 °C.

tures emerged due to the diffusion and secondary organization of BN spherical balls into larger islands. At 900 °C however, only sub-micron spherical BN balls were formed, the absence of larger secondary structures may be due to their fragmentation. The compositional analysis of the BN nanoballs synthesized at 900 °C revealed that these are actually BC_xN ($x \sim 0.15$). The mirror-shine, smooth BC_xN films (r.m.s roughness ~ 2.6 nm) deposited at 900 °C may be useful as a chemically inert coating for tribological applications.

References

[1] R. T. Paine and C. K. Narula, Chem. Rev. **90**, 73 (1990).
[2] K. P. Loh, M. Nishitani-Gamo, I. Sakaguchi, T. Taniguchi, and T. Ando, Appl. Phys. Lett. **72**, 3023 (1998).
[3] K. P. Loh, I. Sakaguchi, M. Nishitani-Gamo, S. Tagawa, T. Sugino, and T. Ando, Appl. Phys. Lett. **74**, 28 (1999).
[4] K. P. Loh, I. Sakaguchi, M. Nishitani-Gamo, T. Taniguchi, and T. Ando, Diam. Relat. Mater. **8**, 781 (1999).
[5] A. Nagashima, N. Tejiman. Y. Gamouy, T. Kawai, and C. Oshima, Phys. Rev. Lett. **75**, 3918 (1995).
[6] E. Rokuta, Y. Hasegawa, K. Suzuki, Y. Gamou, C. Oshima, and A. Nagashima, Phys. Rev. Lett. **79**, 4609 (1997).
[7] W. Auwarter, T. J. Kreutz, T. Greber, and J. Osterwalder, Surf. Sci. **429**, 229 (1999).
[8] G. B. Grad, P. Blaha, K. Schwarz, W. Auwarter, and T. Greber, Phys. Rev. B **68**, 085404 (2003).
[9] M. Corso, W. Auwärter, M. Muntwiler, A. Tamai, T. Greber, and J. Osterwalder, Science **303**, 217 (2004).
[10] J. Tersoff and R. M. Tromp, Phys. Rev. Lett. **70**, 2782 (1993).
[11] V. Afanasev, A. Stesman, and C. Harris, Mater. Sci. Forum **264–268**, 857 (1998).
[12] B. Hoenetz, H. Michel, and J. Halbritter, J. Mater. Res. **9**, 3088 (1994).
[13] M. Hollering, F. Maier, N. Sieber, M. Stammler, J. Ristein, L. Ley, A. P. J. Stampfl, J. D. Riley, R. C. G. Leckey, F. P. Leisenberger, and F. P. Netzer, Surf. Sci. **442**, 531 (1999).
[14] X. N. Xie and K. P. Loh, J. Appl. Phys. **92**, 5173 (2002).
[15] N. Onojima, J. Suda, and H. Matsunami, Appl. Phys. Lett. **80**, 76 (2002).

Dr. Kian Ping Loh is currently an Assistant Professor at the Department of Chemistry of the National University of Singapore. He obtained his D. Phil. from University of Oxford in 1997 and spent one and a half year at the National Institute for Research in Material Science between 1997 and 1998. His background is in surface science and synthesis of nanomaterials. He researched on the growth of diamond and boron nitride thin films and is currently fabricating nanocrystalline diamond and boron nitride nanotubes.